THE JOURNAL OF PHYSICAL CHEMISTRY Letters

Letter

pubs.acs.org/JPCL

Femtosecond Photoelectron Imaging of Aligned Polyanions: Probing Molecular Dynamics through the Electron–Anion Coulomb Repulsion

Daniel. A. Horke, Adam S. Chatterley, and Jan R. R. Verlet*

Department of Chemistry, University of Durham, DH1 3LE Durham, United Kingdom

ABSTRACT: The first time-resolved photoelectron imaging study of a polyanion is presented. Using the alignment induced through resonance excitation, the photoelectron angular distributions can be qualitatively understood in terms of the position of localized excess charges on the molecular skeleton, which influence the photoemission dynamics. Pump–probe experiments are used to demonstrate that the photoelectron angular distribution is also sensitive to molecular dynamics. This is shown here for the rotational dynamics of a polyanion, in which the photoelectron anisotropy tracks the rotational coherence as it dephases. The methodology can in principle be applied to general molecular dynamics in large polyanions, providing a new route to studying ultrafast structural dynamics in complex gas-phase systems.

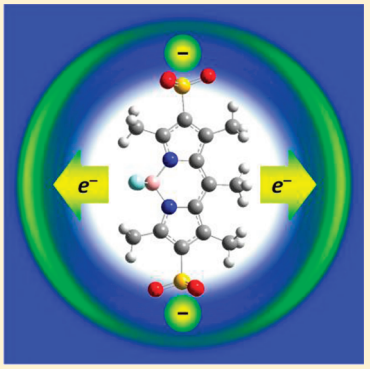

SECTION: Dynamics, Clusters, Excited States

Polyanions are common in condensed phases, where the interaction with neighboring species stabilizes the inherent intramolecular Coulombic repulsion. When isolated in the gas-phase, this repulsion renders many polyanions unstable, either with respect to electron loss or fragmentation.[1−4] Despite this instability, polyanions also possess a dynamic stability due to the repulsive Coulomb barrier (RCB) that arises from a balance between the short-range attraction and the long-range repulsion between an electron and anion (see Figure 1a).[5−10] The RCB is generally not isotropic and depends on the location of the excess charges within the molecular framework. While for anions or neutrals the photoelectron angular distribution (PAD) is determined by the interference of the partial photoelectron waves, in polyanions, it has been shown through photoelectron (PE) imaging[11−13] that the shape of the RCB strongly influences the outgoing electrons.[14−16] In this Letter, we report the first time-resolved PE imaging study of a polyanion. It is shown that the PAD can be qualitatively understood based on the photoinduced alignment of the polyanion. Moreover, the PADs are shown to be sensitive to molecular rotational dynamics. These observations suggest that time-resolved PE imaging of polyanions may provide an elegant route to discerning large-amplitude structural dynamics in the gas-phase, with femtosecond resolution.

In PE imaging, the outgoing electron is captured in the laboratory frame. Relating the photoemission process to the molecular frame through molecular alignment has been demonstrated using a number of methods.[17−20] Here, we align a dianion in the laboratory frame using a well-defined molecular transition, from an initial state m to a final state n. If the direction of the transition dipole moment, $\mathbf{d}_{nm}$, is known,

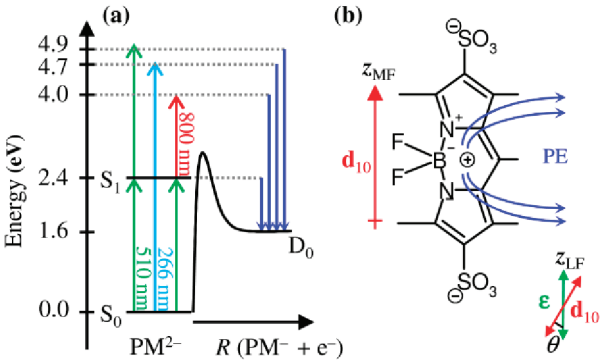

Figure 1. (a) Energy level diagram of PM^{2-}, showing the repulsive Coulomb barrier (RCB) to photodetachment and the excitation and photodetachment schemes used. (b) The structure of PM^{2-}, with the transition dipole moment for $S_1 \leftarrow S_0$ excitation, $\mathbf{d}_{10}$, shown, which defines the molecular frame z-axis, z_{MF}. Also shown is the polarization vector of the excitation field, $\boldsymbol{\varepsilon}$, which defines the laboratory frame z-axis, z_{LF}. Excitation of PM^{2-} results in the relative alignment of z_{MF} to z_{LF} with an angle θ, according to a $\cos^2\theta$ distribution. A qualitative sketch indicating the direction of the outgoing photoelectrons (PEs) is shown as blue arrows, which is determined by the Coulombic repulsion from the remaining charges on the molecule.

excitation with linearly polarized light, $\boldsymbol{\varepsilon}$, will produce an ensemble of molecules in an excited state, aligned in a $\cos^2\theta$ distribution (where θ is the angle between $\mathbf{d}_{nm}$ and the laser

Received: January 24, 2012
Accepted: March 6, 2012

 © XXXX American Chemical Society dx.doi.org/10.1021/jz3000933 | J. Phys. Chem. Lett. 2012, 3, 834–838

polarization, $\boldsymbol{\varepsilon}$). Because $\boldsymbol{\varepsilon}$ defines the laboratory frame and $\mathbf{d}_{nm}$ the molecular frame, a measurement in the laboratory frame will provide molecular frame information.

As a model system, the laser dye pyrromethene 556 (PM^{2-}) is used.[21,22] Its structure, shown in Figure 1b, is comprised of a central boron-dipyrromethene (BODIPY) chromophore and two terminal SO_3^- groups, where the excess charges are localized. The BODIPY chromophore has been extensively studied.[23,24] It has a strong $S_1 \leftarrow S_0$ transition centered around 2.49 eV (498 nm) in methanol,[25] and $\mathbf{d}_{10}$ is aligned along the z_{MF}-axis, defined in Figure 1b.

Experimentally, isolated PM^{2-} is generated from a 1 mM solution of the PM sodium salt (Exciton) in methanol, using electrospray ionization.[26,27] An ion bunch of mass-selected PM^{2-} is produced by trapping the ions in a radio frequency ion trap. Following trapping, the ion packet is injected into a time-of-flight mass spectrometer at 500 Hz. The ion bunch is then intersected perpendicularly by femtosecond laser pulses at the center of a velocity-map imaging PE spectrometer.[28] Electrons are guided in the direction mutually perpendicular to the ion and laser beams, towards a position-sensitive detector. The position of the PE striking the detector is monitored using a charge-coupled device. The resultant PE images are reconstructed using polar onion peeling to yield the central slice through the 3D PE cloud, providing the PE spectrum and PAD.[29] Femtosecond pulses are derived from a commercial amplified Ti:Sapphire laser system, with a fundamental output at 1.55 eV (800 nm). Femtosecond pulses at 4.66 eV (266 nm) are generated by third harmonic generation. Light at 2.43 eV (510 nm) is produced using an optical parametric amplifier and subsequent frequency mixing of the signal with the fundamental. Pump and probe pulses are delayed relative to each other using a motorized optical delay line, and the temporal resolution, as determined by a cross correlation, is on the order of 140 fs. The intensity of all pulses in the interaction region is on the order of 1×10^{10} W cm^{-2}, and $\boldsymbol{\varepsilon}$ is set to be parallel to the detector and defines the z_{LF}-axis (see Figure 1b). The polarization purity of pump and probe pulses is ~10:1. PE spectra have been calibrated to the known spectrum of I^-, and the spectrometer has a spectral resolution of $\Delta E/E = 5\%$.

Figure 2a shows the PE spectrum taken at 4.66 eV (266 nm). It shows a single PE feature at an electron kinetic energy of eKE ≈ 2.7 eV. From this feature, the adiabatic binding energy of PM^{2-} can be determined to be 1.6 ± 0.2 eV. This is in agreement with ab initio calculations[30,31] that also show that the highest-occupied molecular orbital (HOMO) of PM^{2-} is that of the π-system of the BODIPY chromophore. PE spectroscopy will therefore form a zwitterionic system, in which a hole is left on the BODIPY system and two negative charges are on the terminal SO_3^- groups. The outgoing PE will consequently be influenced by the resultant electrostatic RCB potential. The RCB will be anisotropic with respect to the molecular axis, exhibiting large potential maxima around the SO_3^- groups, while the lowest saddle point in the RCB will be along the plane perpendicular to the molecular axis. There will be influences on the exact shape of the RCB, particularly due to the out-of-plane F atoms and the fact that the system is not symmetric about z_{MF}. These will however be relatively minor compared to the presence of the charged regions of the system.

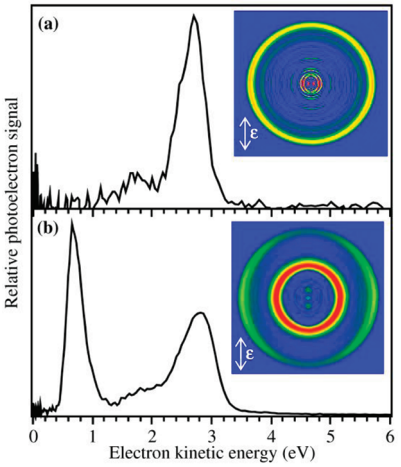

Figure 2. Photoelectron spectrum of PM^{2-} collected at (a) 4.66 (266 nm) and (b) 2.43 eV (510 nm). Shown in the inset is the central slice of the corresponding photoelectron image.

The inset in Figure 2a shows the central slice through the PE Newton sphere. The PE anisotropy can be quantified by fitting the PAD to the well-known expression

$$I(\theta) = \frac{\sigma}{4\pi}\left(1 + \sum_{2n} \beta_n P_n(\cos\theta)\right)$$

where σ is the cross section for detachment, $P_n(\cos\theta)$ are the nth-order Legendre polynomials, and β_n is a measure of the anisotropy.[32] The sum runs over $2n$, where n is the number of photons absorbed. For the one-photon PE image in Figure 2a, $\beta_2 = -0.15 \pm 0.10$, indicating that the PAD is almost isotropic. At first glance, this observation would suggest that the RCB has little or no effect on the outgoing photoelectrons. However, the PEs are collected in the laboratory frame, and if there is no correlation between laboratory and the molecular frames, then experimentally, one cannot determine the effect of the RCB on the outgoing electron. In the experiments by the Wang group,[14,16] this correlation is provided by the dependence of the integral photodetachment cross section on the molecular orientation. The polyanions in their study[14] have a similar overall RCB to PM^{2-} (i.e., a central chromophore and terminal negatively charged groups), but the photodetachment cross section peaks when the molecular axis is aligned with $\boldsymbol{\varepsilon}$. This leads to the observed negative anisotropy parameter as the PE leaves preferentially perpendicular to the molecular axis to avoid the large RCB near the negative charges. For PM^{2-}, the integral cross section appears to be significantly less sensitive to the molecular orientation such that the influence of the RCB cannot be clearly observed. This is reflected in the one-photon detachment from PM^{2-}, where the observed anisotropy following detachment at 266 nm is near isotropic (Figure 2a). Therefore, in order to reliably observe the influence of the RCB on an outgoing photoelectron in PM^{2-}, a connection between the laboratory and molecular frames must be established. This can be achieved through alignment of the molecule in space. Such a methodology is generally applicable to any polyanion, irrespective of variations in the integral photodetachment cross section with respect to the molecular frame, and this is demonstrated here using alignment through a resonant electronic transition.

dx.doi.org/10.1021/jz3000933 | J. Phys. Chem. Lett. 2012, 3, 834–838

Figure 2b shows the PE spectrum taken at $h\nu$ = 2.43 eV (510 nm), resonant with the $S_1 \leftarrow S_0$ transition. The PE spectrum shows features centered at eKE = 0.7 and 2.9 eV. The PE feature at eKE = 0.7 eV arises from absorption of a single photon. We can crudely estimate the lowest RCB by calculating the potential energy of an electron interacting with a system in which we assume a negative point charge on the two SO_3^- groups and a point charge hole on the BODIPY. This yields an outer RCB of 1.3 eV.[33,34] Given the adiabatic binding energy of 1.6 eV, at least 2.9 eV is required to directly detach an electron. Hence, the feature observed at eKE = 0.7 eV must arise from tunneling through the RCB.[5] In solution, the S_1 is highly fluorescent with a quantum yield = 0.98[22] and a nanosecond lifetime,[35] and hence, it is not unreasonable to anticipate that tunneling through the RCB will be a competitive decay pathway for the S_1 state in the gas-phase.[5,36]

The feature at eKE = 2.9 eV is commensurate with the absorption of two photons. This would impart a total of 4.86 eV, extending the PE spectrum by an additional 0.2 eV relative to the PE spectrum taken at 4.66 eV (266 nm) shown in Figure 2a. Importantly, this is a resonance-enhanced two-photon detachment (R2PD) feature as the first photon is resonant with the $S_1 \leftarrow S_0$ transition. This accounts for the large PE signal observed for this feature. Hence, the feature at eKE = 2.9 eV arises from the photodetachment of PM^{2-} in its S_1 state, not the ground S_0 state.

Analysis of the PE image shown in the inset in Figure 2b reveals that the two PE features have very different PADs. Specifically, the tunneling feature is almost isotropic (β_2 = −0.16 ± 0.08), while the R2PD feature is strongly anisotropic (β_2 = −0.60 ± 0.09, β_4 = 0.06 ± 0.10) in the direction perpendicular to $\boldsymbol{\varepsilon}$. As shown by the Wang group, an outgoing PE can be strongly affected by the RCB.[14,16] For PM^{2-}, the R2PD feature arises from the photodetachment from the S_1 state. As this state is prepared by excitation with linearly polarized light, PM^{2-} molecules in the S_1 state will be aligned relative to the z_{LF} with a $\cos^2\theta$ distribution. Hence, any PE generated by absorption of an additional photon will experience a RCB that is aligned in the lab frame. In Figure 1b, $\mathbf{d}_{10}$ is aligned with z_{LF} such that, in a simplistic classical picture, a PE will experience a RCB that forces it in a direction perpendicular to z_{LF}, which leads to the observed $\beta_2 < 0$ anisotropy. The fact that the observed β_4 is close to zero for this feature suggests that the cross section for photodetachment from the S_1 state is also relatively invariant to the molecular alignment.

The tunneling feature at eKE = 0.7 eV shows an almost isotropic PAD, despite the fact that this feature also arises from an aligned distribution of PM^{2-} molecules in the S_1 excited state. However, as this peak is formed by electrons that tunnel and this is a delayed process, molecular dynamics in the excited state may compete with tunneling.

We probe the relaxation dynamics of the S_1 state using time-resolved PE spectroscopy. Population in the S_1 state is prepared via $S_1 \leftarrow S_0$ excitation with a 2.43 eV (510 nm) photon and probed at various delays later using a 1.55 eV (800 nm) photon. The probe is sufficiently energetic to directly detach an electron from the S_1 excited state but insufficient for direct detachment from the S_0 ground state of the dianion. A PE spectrum near the temporal overlap between the two pulses is shown in Figure 3a and shows the additional PE feature centered at eKE = 1.9 eV. This feature is a direct probe of the S_1 state population, and in Figure 3b, we show the integrated PE signal (in 1.6 < eKE < 2.1 eV) as a function of pump−probe delay. The S_1 state

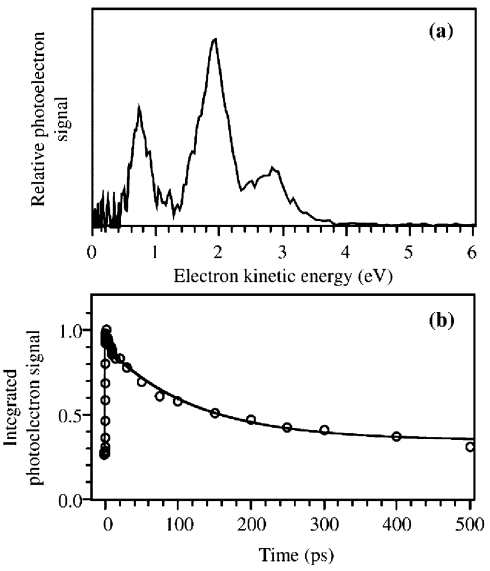

Figure 3. (a) Photoelectron spectrum taken with pump (2.43 eV, 510 nm) and probe (1.55 eV, 800 nm) pulses overlapping, t = 0.5 ps. A large 1 + 1′ detachment feature is observed at eKE = 1.9 eV. (b) Total integrated photoelectron signal of the 1 + 1′ detachment feature, fitted with a single exponential decay, yielding an excited state lifetime of 120 ps.

population shows first-order decay kinetics,[5] and we fit these data with a single exponential decay, yielding a tunneling lifetime of 120 ± 30 ps. The tunneling lifetime is relatively long, and rotational dephasing dynamics are expected to occur on time scales that are significantly faster than this, suggesting that the alignment may be lost before the majority of electrons are ejected from the excited state, thus leading to an isotropic distribution.

The observed PAD for detachment from the S_1 is a measure of the degree of alignment within the ensemble of S_1 excited PM^{2-}, and therefore, the time-resolved PADs can be used to track the rotational dephasing following excitation of the S_1 state. To exclusively monitor the anisotropy of the S_1 state, we have subtracted from each time-resolved PE image an image taken when the probe arrives before the pump ($t < t_0$). Representative central slices through the PE images following such a subtraction are shown in Figure 4a−c for a number of different pump−probe delays. These indicate changes in the PADs with pump−probe delay. These changes can be quantified through the changes in anisotropy parameter $\Delta\beta_2$, as shown in Figure 4d, which have been referenced to the long-time anisotropy that is assumed to be isotropic. When pump and probe pulse are temporally overlapped (t = 0), the anisotropy is maximal at β_2 = −0.53 ± 0.17. Within error, this value agrees with the value obtained from the R2PD feature in the PE spectrum taken at 2.43 eV (510 nm). We note that, although our determination of the absolute β_2 value has a relatively large error, we have shown that we are significantly more sensitive to changes in β_2.[26] As the pump−probe delay increases, the images become more isotropic, reflected as a decrease in the absolute β_2 value. After a few picoseconds, the PADs are almost isotropic and show no further changes at longer delays where only the intensity of the image decreases.

The observed changes in PADs can be rationalized in terms of the dephasing of the rotational coherence initially excited in the S_1 state. Following excitation, a coherent distribution of

dx.doi.org/10.1021/jz3000933 | J. Phys. Chem. Lett. 2012, 3, 834−838

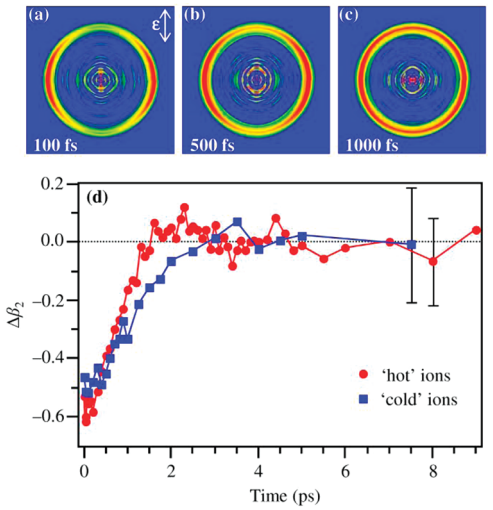

Figure 4. (a–c) Background-subtracted deconvoluted photoelectron images, showing the varying anisotropy as a function of pump–probe delay, for ions prepared hot. (d) Observed change in the photoelectron anisotropy parameter, $\Delta\beta_2$, as a function of pump–probe delay for ions prepared with different amounts of internal energy.

rotational states is excited in the S_1 state, as shown by Felker and Zewail.[37,38] This leads to an aligned distribution at $t = 0$ by virtue of the alignment between $\mathbf{d}_{10}$ and $\boldsymbol{\varepsilon}$. As the rotational coherences evolve, their phases rapidly become scrambled, and the ensemble of S_1 excited PM^{2-} appears isotropically distributed, leading to the observed changes in β_2. As the superposition is coherent, rotational revivals are expected to occur at times determined by the rotational constants of the system.[39] For PM^{2-}, the earliest possible half revival occurs on a time scale that greatly exceeds the observed S_1 lifetime, and therefore, these revivals are not observed experimentally.

The fast dephasing time of the initial ensemble arises from the fact that the ground-state PM^{2-} is intentionally prepared hot and hence a large number of rotational states contribute to the dynamics. The temperature is crudely controlled by the potential used to empty the ion trap and by the buffer gas in the trap. For the current experiments, air was used as a buffer gas, which leads to a substantial heating of ions. Changing the buffer gas to He is expected to reduce the internal energy transferred to the trapped ions by a factor of ~6, bringing the temperature close to 300 K. At this lower temperature, the rotational dynamics slow appreciably, as shown in Figure 4d. This provides strong support for our interpretation of the observed dynamics arising from rotational dephasing, which is determined by the initial rotational distribution of the molecules in the ground state. The observed picosecond time scale for rotational dephasing is in agreement with studies in systems of a similar size.[40]

The key observations here are that the RCB directs the photoelectron emission in polyanions and that PE imaging can be used to qualitatively predict the shape of the RCB. In general, photodetachment is governed by the quantum nature of the outgoing electron, and the PADs are governed by the interference between outgoing partial waves as well as partial wave cross sections. This remains the correct description for understanding the PE emission from polyanions. However, it is also evident that the RCB has a determining influence on the possible directions in which the PE can be ejected; certain regions of space are simply inaccessible as the Coulomb barriers are too high relative to the energy of the ejected electron. Despite its shortcomings, this then provides a simple classical framework in which to qualitatively interpret experimentally observed PADs. The observation of temporal changes in the anisotropy as the molecular alignment in PM^{2-} is lost provides additional support for this conceptual picture. More importantly, the temporal evolution of the PAD suggests that time-dependent changes of the RCB can be used as a probe for the molecular dynamics. This has been demonstrated here for changes in the RCB within the laboratory frame, but it can in principle also be extended to changes in the molecular frame RCB. Because the RCB depends critically on where the excess charges are localized on the molecular frame, the time-resolved PAD provides a crude measure of the structure of the polyanion at a given time following excitation. Time-resolved PE imaging therefore provides a route to measuring structural dynamics on a femtosecond time scale. For example, isomerization dynamics will be reflected in dynamic changes in PADs as there can be large changes in the relative location of the excess negative charges during such structural changes. These experiments are currently underway in our laboratory.

AUTHOR INFORMATION

Corresponding Author

*E-mail: j.r.r.verlet@durham.ac.uk.

Notes

The authors declare no competing financial interest.

ACKNOWLEDGMENTS

This work has been supported by the EPSRC (EP/D073472/1) and Durham University. A.S.C. is funded by the Leverhulme Trust.

REFERENCES

(1) Boldyrev, A. I.; Gutowski, M.; Simons, J. Small Multiply Charged Anions as Building Blocks in Chemistry. *Acc. Chem. Res.* **1996**, *29*, 497–502.
(2) Dreuw, A.; Cederbaum, L. S. Multiply Charged Anions in the Gas Phase. *Chem. Rev.* **2002**, *102*, 181–200.
(3) Scheller, M. K.; Compton, R. N.; Cederbaum, L. S. Gas-Phase Multiply Charged Anions. *Science* **1995**, *270*, 1160–1166.
(4) Wang, X.-B.; Wang, L.-S. Photoelectron Spectroscopy of Multiply Charged Anions. *Annu. Rev. Phys. Chem.* **2009**, *60*, 105–126.
(5) Ehrler, O. T.; Yang, J.-P.; Sugiharto, A. B.; Unterreiner, A. N.; Kappes, M. M. Excited State Dynamics of Metastable Phthalocyanine–Tetrasulfonate Tetra-Anions Probed by Pump/Probe Photoelectron Spectroscopy. *J. Chem. Phys.* **2007**, *127*, 184301.
(6) Ehrler, O. T.; Weber, J. M.; Furche, F.; Kappes, M. M. Photoelectron Spectroscopy of C_{84} Dianions. *Phys. Rev. Lett.* **2003**, *91*, 113006.
(7) Matheis, K.; Joly, L.; Antoine, R.; Lepine, F.; Bordas, C.; Ehrler, O. T.; Allouche, A. R.; Kappes, M. M.; Dugourd, P. Photoelectron Spectroscopy of Gramicidin Polyanions: Competition between Delayed and Direct Emission. *J. Am. Chem. Soc.* **2008**, *130*, 15903–15906.
(8) Wang, L.-S.; Ding, C.-F.; Wang, X.-B.; Nicholas, J. B. Probing the Potential Barriers and Intramolecular Electrostatic Interactions in Free Doubly Charged Anions. *Phys. Rev. Lett.* **1998**, *81*, 2667–2670.
(9) Wang, X.-B.; Ding, C.-F.; Wang, L.-S. Photodetachment Spectroscopy of a Doubly Charged Anion: Direct Observation of the Repulsive Coulomb Barrier. *Phys. Rev. Lett.* **1998**, *81*, 3351–3354.
(10) Wang, X.-B.; Wang, L.-S. Observation of Negative Electron-Binding Energy in a Molecule. *Nature* **1999**, *400*, 245–248.

(11) Mabbs, R.; Grumbling, E. R.; Pichugin, K.; Sanov, A. Photoelectron Imaging: An Experimental Window into Electronic Structure. *Chem. Soc. Rev.* **2009**, *38*, 2169−2177.
(12) Stolow, A.; Bragg, A. E.; Neumark, D. M. Femtosecond Time-Resolved Photoelectron Spectroscopy. *Chem. Rev.* **2004**, *104*, 1719−1758.
(13) Verlet, J. R. R. Femtosecond Spectroscopy of Cluster Anions: Insights into Condensed-Phase Phenomena from the Gas-Phase. *Chem. Soc. Rev.* **2008**, *37*, 505−517.
(14) Ning, C.-G.; Dau, P. D.; Wang, L.-S. Guiding Electron Emissions by Excess Negative Charges in Multiply Charged Molecular Anions. *Phys. Rev. Lett.* **2010**, *105*, 263001.
(15) Xing, X. P.; Wang, X. B.; Wang, L. S. Imaging Intramolecular Coulomb Repulsions in Multiply Charged Anions. *Phys. Rev. Lett.* **2008**, *101*, 083003.
(16) Xing, X.-P.; Wang, X.-B.; Wang, L.-S. Photoelectron Angular Distribution and Molecular Structure in Multiply Charged Anions. *J. Phys. Chem. A* **2008**, *113*, 945−948.
(17) Holmegaard, L.; Hansen, J. L.; Kalhoj, L.; Louise Kragh, S.; Stapelfeldt, H.; Filsinger, F.; Kupper, J.; Meijer, G.; Dimitrovski, D.; Abu-samha, M.; et al. Photoelectron Angular Distributions from Strong-Field Ionization of Oriented Molecules. *Nat. Phys.* **2010**, *6*, 428−432.
(18) Lee, K. F.; Villeneuve, D. M.; Corkum, P. B.; Stolow, A.; Underwood, J. G. Field-Free Three-Dimensional Alignment of Polyatomic Molecules. *Phys. Rev. Lett.* **2006**, *97*, 173001.
(19) Lu, Z.; Continetti, R. E. Alignment of a Molecular Anion Via a Shape Resonance in Near-Threshold Photodetachment. *Phys. Rev. Lett.* **2007**, *99*, 113005.
(20) Stapelfeldt, H.; Seideman, T. Colloquium: Aligning Molecules with Strong Laser Pulses. *Rev. Mod. Phys.* **2003**, *75*, 543−557.
(21) Guggenheimer, S. C.; Boyer, J. H.; Thangaraj, K.; Shah, M.; Soong, M.-L.; Paviopoulos, T. G. Efficient Laser Action from Two Cw Laser-Pumped Pyrromethene−BF_2 Complexes. *Appl. Opt.* **1993**, *32*, 3942−3943.
(22) Pavlopoulos, T. G.; Shah, M.; Boyer, J. H. Efficient Laser Action from 1,3,5,7,8-Pentamethylpyrromethene-BF_2 Complex and Its Disodium 2,6-Disulfonate Derivative. *Opt. Commun.* **1989**, *70*, 425−427.
(23) López Arbeloa, F.; Bañuelos, J.; Martínez, V.; Arbeloa, T.; López Arbeloa, I. Structural, Photophysical and Lasing Properties of Pyrromethene Dyes. *Int. Rev. Phys. Chem.* **2005**, *24*, 339−374.
(24) Loudet, A.; Burgess, K. Bodipy Dyes and Their Derivatives: Syntheses and Spectroscopic Properties. *Chem. Rev.* **2007**, *107*, 4891−4932.
(25) Assor, Y.; Burshtein, Z.; Rosenwaks, S. Spectroscopy and Laser Characteristics of Copper-Vapor-Laser Pumped Pyrromethene-556 and Pyrromethene-567 Dye Solutions. *Appl. Opt.* **1998**, *37*, 4914−4920.
(26) Lecointre, J.; Roberts, G. M.; Horke, D. A.; Verlet, J. R. R. Ultrafast Relaxation Dynamics Observed through Time-Resolved Photoelectron Angular Distributions. *J. Phys. Chem. A* **2010**, *114*, 11216−11224.
(27) Horke, D. A.; Verlet, J. R. R. Time-Resolved Photoelectron Imaging of the Chloranil Radical Anion: Ultrafast Relaxation of Electronically Excited Electron Acceptor States. *Phys. Chem. Chem. Phys.* **2011**, *13*, 19546−19552.
(28) Eppink, A. T. J. B.; Parker, D. H. Velocity Map Imaging of Ions and Electrons Using Electrostatic Lenses: Application in Photoelectron and Photofragment Ion Imaging of Molecular Oxygen. *Rev. Sci. Instrum.* **1997**, *68*, 3477−3484.
(29) Roberts, G. M.; Nixon, J. L.; Lecointre, J.; Wrede, E.; Verlet, J. R. R. Toward Real-Time Charged-Particle Image Reconstruction Using Polar Onion-Peeling. *Rev. Sci. Instrum.* **2009**, *80*, 053104.
(30) Calculations performed using the Gaussian09 software package [31]. Energies and optimizations were calculated at the DFT/B3LYP/6-311++g(2d,2p) level. The vertical detachment energy was calculated as 1.95 eV and the adiabatic detachment energy as 1.79 eV. The HOMO of the dianion is located on the BODIPY chromophore.
(31) Frisch, M. J.; Trucks, G. W.; Schlegel, H. B.; Scuseria, G. E.; Robb, M. A.; Cheeseman, J. R.; Scalmani, G.; Barone, V.; Mennucci, B.; Petersson, G. A. et al. *Gaussian09*, revision A.02; Gaussian, Inc.: Wallingford, CT, 2009.
(32) Cooper, J.; Zare, R. N. Angular Distribution of Photoelectrons. *J. Chem. Phys.* **1968**, *48*, 942−943.
(33) Horke, D. A.; Chatterley, A. S.; Verlet, J. R. R. *Phys. Rev. Lett.* **2012**, *108*, 083003.
(34) Marcum, J. C.; Weber, J. M. Electronic Photodissociation Spectra and Decay Pathways of Gas-Phase $IrBr_6^{2-}$. *J. Chem. Phys.* **2009**, *131*, 194309−194308.
(35) Pardoen, J. A.; Lugtenburg, J.; Canters, G. W. Optical Properties of Pyrromethene Derivatives. Possible Excited-State Deactivation through Proton Tunneling. *J. Phys. Chem.* **1985**, *89*, 4272−4277.
(36) Wang, X.-B.; Ding, C.-F.; Wang, L.-S. Electron Tunneling through the Repulsive Coulomb Barrier in Photodetachment of Multiply Charged Anions. *Chem. Phys. Lett.* **1999**, *307*, 391−396.
(37) Baskin, J. S.; Felker, P. M.; Zewail, A. H. Purely Rotational Coherence Effect and Time-Resolved Sub-Doppler Spectroscopy of Large Molecules. II. Experimental. *J. Chem. Phys.* **1987**, *86*, 2483−2499.
(38) Felker, P. M.; Zewail, A. H. Purely Rotational Coherence Effect and Time-Resolved Sub-Doppler Spectroscopy of Large Molecules. I. Theoretical. *J. Chem. Phys.* **1987**, *86*, 2460−2482.
(39) Felker, P. M.; Baskin, J. S.; Zewail, A. H. Rephasing of Collisionless Molecular Rotational Coherence in Large Molecules. *J. Phys. Chem.* **1986**, *90*, 724−728.
(40) Blokhin, A.; Gelin, M.; Khoroshilov, E.; Kryukov, I.; Sharkov, A. Dynamics of Optically Induced Anisotropy in an Ensemble of Asymmetric Top Molecules in the Gas Phase. *Opt. Spectrosc.* **2003**, *95*, 346−352.